

LIGAND-ASSISTED ADSORPTION OF CR(III) IONS ON MODIFIED NANO-ADSORBENTS**Mohd. Tousif Ahmed¹ and Naseem^{2*}**¹ Research Scholar, Department of Pharmaceutical Chemistry, Telangana University, Nizamabad-503322, India² Professor, Department of Pharmaceutical Chemistry, Telangana University, Nizamabad-503322, India²naseemprof695@gmail.com**ABSTRACT**

The integration of natural organic acids with micro-adsorbents has been shown to significantly enhance the adsorption efficiency of Cr(III) ions. Within the domain of nano-adsorbents, incorporating natural organic acids has demonstrated a notable improvement in Cr (III) ions adsorption properties, yielding an increase up to 6.15% compared to micro-adsorbents. Notably, the highest adsorption capacity was observed in the L-Glutamic acid-infused Graphene-oxide system, reaching 1012.03±1.02 ppm, representing an 8.9% enhancement over the non-infused graphene oxide control. In the arena of thermal metal ion desorption processes, nano-adsorbents have exhibited significantly enhanced regenerative capacity, particularly when infused with L-Glutamic acid, resulting in an increase up to 5.8 times. Furthermore, electrolytic desorption of Cr(III) ions from organic acid-infused nano-adsorbents demonstrated a notable increase up to 13.2%. The highest desorption efficiency was observed in the L-Glutamic acid-infused Graphene-oxide system, achieving a reduction of 139.93 ppm in Cr(III) ions concentration. This enhanced efficacy can be ascribed to the electrolytically inducible metal-ligand interaction facilitated by the multifunctional conformational diversity of L-Glutamic acid, underscoring its pivotal role in augmenting the desorption process. The metal-ligand interactions are further corroborated by mass spectrum analysis, particularly by the peaks at m/z: 434.01 and 435.17, which strongly support the prevalence of Cr-L-glutamic acid connections over graphene-oxide. In conclusion, the findings of this study offer valuable insights for designing and developing efficient strategies for the remediation of Cr(III) contaminants from water samples, with a focus on ensuring human and ecological safety.

Index Terms – Adsorption, Desorption, Ligands.

INTRODUCTION

Chromium contaminants are widely recognized as potent human carcinogens, particularly linked to lung and respiratory organ cancers, posing a significant concern due to their slow degradation and enduring presence in soil and water [1,2]. Their persistence in the environment heightens the risk of exposure to organisms and potential bioaccumulation in food chains. Several chromium complexes actively participate in cellular processes, leading to DNA mutations and cellular damage, culminating in cancer and other genetic disorders [3]. Industrial activities such as wood preservation, leather tanning, and chrome plating are major contributors to Cr(VI) pollution in soil and groundwater [4]. Additionally, natural phenomena like rock weathering and volcanic eruptions also contribute to its presence in the environment [5].

Cr(III) ions nonetheless provide certain potential risks to human health and the environment, although being widely regarded as less dangerous than their hexavalent equivalent, Cr(VI). Cr(III) ions are proven to be potentially hazardous contaminants to biological and ecological systems in macroscopic quantities [6]. Under permissible levels, Cr(III) ions are generally thought to be safer; nonetheless, microbial interventions and other geological processes may cause Cr(III) to oxidize into dangerous Cr(VI) ions.[7]

To protect public health, preserve environmental integrity, and ensure compliance with safety and regulatory standards, it is essential to remove chromium deposits from water bodies. Nano-adsorbents are efficiently used in remediation techniques for heavy metal ion contamination and their effectiveness is further enhanced under the presence of certain ligand molecules which facilitates the adsorption mechanism [8]. Furthermore, the regeneration of nano-adsorbents presents difficulties because of the formation of irreversible direct chemical bonds between metal ions and nanoparticles. Regeneration, crucial for sustainable utilization, faces hindrances

due to these interactions, diminishing the efficacy of conventional techniques. Nonetheless, progress in structurally modifying nanomaterials via customized synthetic pathways holds potential for improving regeneration capabilities. Despite the anticipated advantages, such modifications are frequently considered impractical and costly, underscoring the necessity for additional research into cost-effective and feasible strategies to tackle the regeneration hurdles of nano-adsorbents [9].

This research delves into the potential of ligand-assisted adsorption for removing chromium (III) ions from water. Using various naturally occurring carboxylic acid ligands and diverse experimental conditions, we systematically evaluated their effectiveness in capturing Cr(III). Our study also introduces a novel approach for both adsorbing and desorbing Cr(III) ions using ligands. Over time, adsorbents typically become saturated with metal ions, hindering their performance. Desorption offers a solution by regenerating the adsorbent for repeated use. Additionally, it allows recovery of the metal ions, minimizing the need for continual adsorbent replacement, potentially leading to cost savings in large-scale water treatment [10, 11]. Building on recent advancements in developing adsorbents with improved desorption properties for optimized water treatment [12], we explored both thermal and electrolytic methods to understand the interactions between the Cr(III) ions and the ligand-assisted adsorbent.

In this research, we investigate the interaction between metal ions and ligands through mass spectral analysis, elucidating the formation and characterization of metal-ligand complexes. Concurrently, we assess the adsorption mechanism employing experimental isotherms at varying metal ion concentrations, providing insights into the adsorption capacity and affinity of the adsorbent. Additionally, we explore the impact of temperature on the adsorption process to discern its thermodynamic characteristics. By integrating mass spectral analysis, experimental isotherms, and temperature effect evaluation, we aim to comprehensively understand the dynamics of metal ion-ligand interactions and the underlying mechanisms governing adsorption, thereby contributing to the advancement of adsorption technology and environmental remediation strategies.

EXPERIMENTAL

A. Metal ion Adsorption studies:

A solution containing Cr(III)Cl₃.6H₂O salt at a concentration of 250 ppm in double distilled water of analytical grade was prepared. Next, 1 gram of adsorbent material underwent impregnation with naturally occurring organic acids, each prepared separately by dissolving 0.10 grams of the acids in 10 mL of specific solvents: ethyl acetate for stearic acid, hot water for glutamic acid, water for citric acid, and ethanol for nicotinic acid. The impregnation process involved agitating the solution with the adsorbent under probe sonication (using Labman Automatic PRO 250) at a frequency of 20 KHz for 6 hours. The acid-infused adsorbent was then exposed to 50 mL of the 250 ppm metal solution and mechanically stirred for 1 hour before being left at room temperature for 24 hours. After filtration, the adsorbents underwent three washes with distilled water and were subsequently dried in a hot air oven at 60°C for 12 hours. The adsorbent was then leached with 2% HNO₃, and the absorbed metal content was determined using Atomic Absorption Spectroscopy (AAS) employing Thermo-Scientific iCE 3000 series Equipment. The same experimental conditions were maintained for analyzing Langmuir isotherm behavior and evaluating the effect of temperature on adsorption across different temperatures and concentrations.

B. Metal ion Desorption Studies:

To explore the thermal desorption process, 1.0 gram of pre-adsorbed adsorbent sample was placed in a 250 mL beaker containing 200 mL of analytical grade distilled water and subjected to a thermostatic chamber (TMAX-80F) set to 95°C for 1 hour. Following this, the adsorbent was separated via filtration and dried in a hot-air oven at a controlled temperature of 60°C for 1 hour before undergoing analysis for chromium content using AAS. In contrast, for the electrolytic-induced desorption process, 1.0 gram of pre-adsorbed adsorbent sample was placed in a 250 mL beaker with 200 mL of analytical grade distilled water and positioned in a thermostatic chamber (TMAX-80F) at 25°C. Two platinum electrodes were immersed into the solution and connected to a DC battery with a potential difference of 3.0 V for approximately 6 hours. Subsequently, the adsorbent sample was filtered,

dried in a hot-air oven at a regulated temperature of 60°C for 1 hour, and then analyzed for chromium content using AAS.

RESULTS AND DISCUSSIONS

A. Metal adsorption studies:

Liagand-assisted activation of adsorbents provides transpicuous elevation in adsorbability in most of cases depending on the chemical and structural affinities.

Table I. Adsorption Of Cr(III) Ion On Various Pre-Designed Micro-Adsorbent Systems.

Micro Adsorbent System	Adsorption of Cr (III) in ppm
Montmorillonite Clay	941.26±1.25
Silica Gel-60	841.6±1.55
Activated Charcoal	951.1±0.52
Montmorillonite Clay-Stearic Acid	907.06±2.73
Montmorillonite Clay-Citric Acid	970.43±0.66
Montmorillonite Clay-Nicotinic Acid	968.26±0.56
Montmorillonite Clay-L-Glutamic Acid	988.5±0.95
Silica Gel-60-Stearic Acid	818.23±1.59
Silica Gel-60-Citric Acid	841.3±1.15
Silica Gel-60-Nicotinic Acid	846.96±1.81
Silica Gel-60-L-Glutamic Acid	871.40±0.62
Activated Charcoal-Stearic Acid	945.4±3.47
Activated Charcoal-Citric Acid	956.46±1.17
Activated Charcoal-Nicotinic Acid	959.56±1.10
Activated Charcoal-L-Glutamic Acid	996.7±1.44

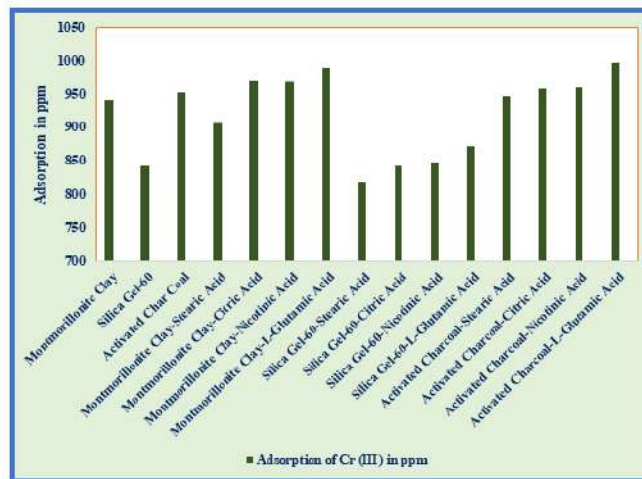


Figure 1. Adsorption Pattern Of Cr(III) On Various Pre-Activated Micro-Adsorbents.

The inclusion of natural organic acids in conjunction with micro-adsorbents has been demonstrated to enhance the adsorption efficiency of Cr(III) by up to 5%, although stearic acid exhibits a unique behavior, leading to a decrease in adsorption capacity by 3.6%. Among the various systems studied, the Activated-charcoal-L-Glutamic acid system showed the highest adsorption capacity, with remarkable adsorption of Cr(III) reaching 996.7±1.44 ppm (**Figure 1**).

The positive results achieved with micro adsorbents have laid a foundation for further exploration at the nano level. By conducting analogous experiments on nano-scale adsorbents, we aim to delve deeper into the intricacies of adsorption mechanisms and evaluate the potential advantages of utilizing smaller particles in adsorption systems. Micro adsorbents have demonstrated their effectiveness in capturing and retaining target substances. However, the shift to nano adsorbents is driven by the anticipation that their smaller size may offer unique advantages, such as increased surface area, enhanced reactivity, and improved adsorption kinetics. These attributes could potentially lead to more efficient and rapid adsorption processes, making nano adsorbents a promising avenue for advancing adsorption technology.

Table II. Adsorption Of Cr(III) On Various Pre-Designed Nano-Adsorbent Systems.

Nano-Adsorbent System	Adsorption of Cr (III) in ppm
Nano-Montmorillonite Clay (50-100nm)	961.63±0.50
SiO ₂ -NP(50-100)	857.56±0.41
Graphene-oxide (3-6 nm)	971.06±0.90
Nano Montmorillonite Clay-Stearic Acid	949.10±1.00
Nano Montmorillonite Clay-Citric Acid	968.36±0.64
Nano Montmorillonite Clay-Nicotinic Acid	987.80±1.12
Nano Montmorillonite Clay-L-Glutamic Acid	1010.06±0.90
SiO ₂ NP-Stearic Acid	860.50±0.60
SiO ₂ NP-Citric Acid	861.90±0.20

SiO ₂ NP-Nicotinic Acid	869.23±0.41
SiO ₂ NP-L-Glutamic Acid	901.66±0.45
Graphene-Oxide-Stearic Acid	966.66±1.47
Graphene-Oxide-Citric Acid	988.10±0.91
Graphene-Oxide-Nicotinic Acid	996.50±1.21
Graphene-Oxide-L-Glutamic Acid	1058.00±1.01

Adsorption of Cr(III) by nano adsorbents showed identical trends with micro-adsorption systems but showed elevated adsorption values (**Table 2**).

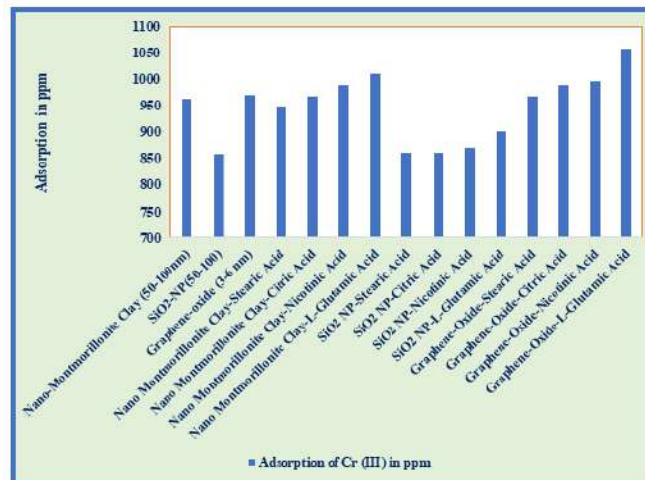


Figure 2. Adsorption Pattern Of Cr(III) On Various Pre-Activated Nano-Adsorbents.

It is evident from the study that, Graphene exhibits higher metal ion adsorption compared to other nano adsorbents due to its unique structural and chemical properties (**Figure 2**). In the realm of Nano-adsorbents, the integration of natural organic acids has shown a notable enhancement in the adsorption properties of Cr(III), resulting in an increase up to 6.15% compared to micro-adsorbents, although stearic acid exhibited a marginal decrease owing to its hydrophobic nature, which attenuates metal ion-ligand interactions. Remarkably, the highest adsorption capacity was observed in the L-Glutamic acid-infused Graphene-oxide system, reaching 1012.03±1.02 ppm, which marks an 8.9% improvement over the non-infused graphene oxide control.

Chemical functionalization of graphene-oxide can be used to add certain functional groups that improve metal ion adsorption. By adding sites that may create strong coordination bonds with metal ions, functionalization modifies the surface chemistry of graphene and increases its adsorption effectiveness. In addition to this, because of conformational flexibility, graphene may take on several conformations, such as taking on the size and shape of metal ions. By maximizing the adsorption capacity, this flexibility makes sure that a greater percentage of the graphene surface is in touch with the metal ions. Graphene also has ion-exchange capabilities, metal ions can swap places with ions from the surrounding solution. Graphene's total metal ion adsorption capability is increased by this dynamic process.

B. Metal Desorption Studies:

Metal ion desorption helps regenerate the adsorbent, making it available for reuse. Moreover, desorption enables the recovery of metal ions, reducing the need for constant replacement of adsorbents.

In the current research Metal desorption was carried out under TWO conditions;

1. Thermal Desorption at 95°C for 1 hour.
2. Electrochemical Desorption using 3.0 V for 6 hours.

Thermal desorption studies:

Thermal-induced desorption involves raising the temperature of the adsorbent-metal ion complex, which increases the kinetic energy of the system. The increased energy facilitates the breaking of metal-adsorbent bonds, leading to the release of metal ions into the solution. The desorption efficiency is influenced by the temperature applied during the thermal regeneration process [13].

Table III. Thermal Desorption Of Cr(III) From Various Pre-Designed Nano-Adsorbent Systems.

Nano Adsorbent System	Adsorption of Cr(III) in ppm after Thermal Treatment in aqueous Conditions	Desorption in ppm
Nano-Montmorillonite Clay (50-100nm)	920.66±0.55	40.97
SiO ₂ -NP(50-100)	817.93±1.87	39.63
Graphene-oxide (3-6 nm)	961.03±0.96	10.03
Nano Montmorillonite Clay-Stearic Acid	901.33±0.70	47.76
Nano Montmorillonite Clay-Citric Acid	939.73±0.55	28.63
Nano Montmorillonite Clay-Nicotinic Acid	934.3±0.52	53.50
Nano Montmorillonite Clay-L-Glutamic Acid	937.13±0.58	72.93
SiO ₂ NP-Stearic Acid	800.56±0.41	59.93
SiO ₂ NP-Citric Acid	834.7±0.20	27.20
SiO ₂ NP-Nicotinic Acid	824.69±0.65	44.54
SiO ₂ NP-L-Glutamic Acid	837.83±0.70	63.83
Graphene-Oxide-Stearic Acid	946.86±1.06	19.80
Graphene-Oxide-Citric Acid	957.93±0.15	30.16
Graphene-Oxide-Nicotinic Acid	951.43±0.77	45.06
Graphene-Oxide-L-Glutamic Acid	989.96±0.20	68.03

In the context of thermal metal ion desorption processes, the regenerative capacity of nano-adsorbents exhibited a significant enhancement, particularly when infused with L-Glutamic acid, resulting in an increase of up to 5.8 times. Notably, the Graphene-oxide-L-Glutamic acid system demonstrated the highest desorption efficiency, with a remarkable reduction of 58.00 ppm in Cr(III) concentration, highlighting the effectiveness of this combination in facilitating the desorption process (**Figure 3**).

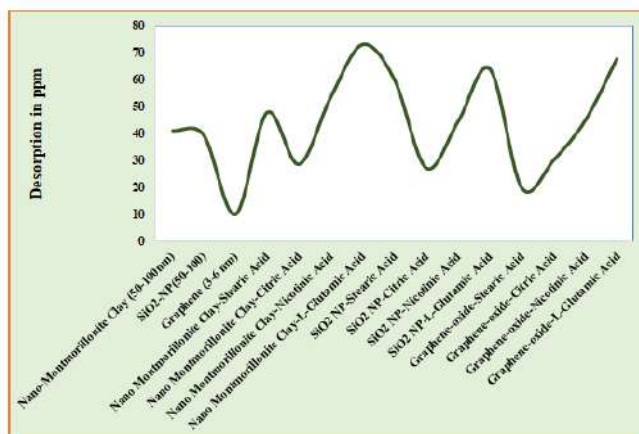


Figure 3. Desorption Patterns Of Cr(III) Under Thermal Conditions.

Electrolytic Induced Desorption Studies:

Applying an electric field to an ion-containing system is known as electrolytic induction, and it may have a big impact on how quickly metal ions desorb from adsorbents.

Electrolytic induction can enhance the desorption of metal ions by providing an electric field that promotes the movement of ions away from the adsorbent surface . The application of an electric field can increase the mobility of metal ions in solution, reducing their affinity for the adsorbent surface and facilitating desorption but the Electrolytic induction allows for selective desorption of specific metal ions based on their electrochemical properties, providing a controlled and targeted approach. Depending on the system design, electrolytic induction can offer energy-efficient desorption methods compared to traditional thermal or chemical regeneration processes [14].

Table IV. Electrolytic Desorption Patterns Of Cr(III) From Pre-Activated Nano-Adsorbents.

Nano Adsorbent System	Adsorption of Cr(III) in ppm after Electrolytic induction in aqueous Conditions	Desorption in ppm
Nano-Montmorillonite Clay (50-100nm)	907.76±0.35	53.86
SiO ₂ -NP(50-100)	727.6±1.60	129.96
Graphene-Oxide (3-6 nm)	954.56±1.52	16.50
Nano Montmorillonite Clay-Stearic Acid	891.73±1.00	57.36
Nano Montmorillonite Clay-Citric Acid	902.46±0.66	65.90
Nano Montmorillonite Clay-Nicotinic Acid	921.1±0.52	66.70
Nano Montmorillonite Clay-L-Glutamic Acid	898.93±1.05	111.13
SiO ₂ NP-Stearic Acid	794.8±0.36	65.70
SiO ₂ NP-Citric Acid	820.96±0.96	40.93
SiO ₂ NP-Nicotinic Acid	816.2±0.60	53.03
SiO ₂ NP-L-Glutamic Acid	809.6±0.95	92.06

Graphene-Oxide-Stearic Acid	927.26±0.47	39.40
Graphene-Oxide-Citric Acid	937.8±0.36	50.30
Graphene-Oxide-Nicotinic Acid	945.6±0.36	50.90
Graphene-Oxide-L-Glutamic Acid	918.06±1.05	139.93

The electrolytic desorption of Cr(III) ions from organic acid-infused nano-adsorbents exhibited a notable increase of up to 13.2%. Notably, electrolytic desorption proved to be more effective than thermal desorption, particularly evident when nano-adsorbents were infused with L-Glutamic acid. The highest desorption efficiency was observed in the L-Glutamic acid infused Graphene-oxide system, achieving a reduction of 139.93 ppm in Cr(III) concentration. This efficacy can be attributed to the electrolytically inducible metal-ligand interaction facilitated by the multifunctional conformational diversity of L-Glutamic acid, emphasizing its role in enhancing the desorption process (**Figure 4**).

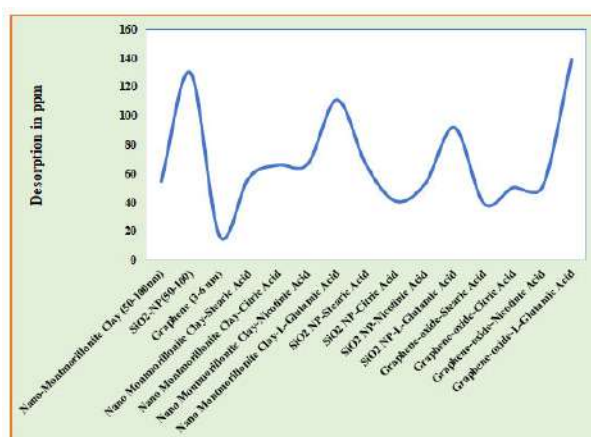


Figure 4. Desorption Patterns Of Cr(III) Under Electrolytic Conditions.

C. Mass Spectrometric Analysis:

The application of mass spectrometry (MS), a potent analytical method, has completely changed our comprehension of metal-ligand interactions. Electrospray ionisation (ESI), one of the several ionisation methods available, has shown to be an especially useful tool for understanding these intricate systems.

When it comes to maintaining non-covalent interactions—like those between metal ions and ligands—ESI is exceptional at ionisation. This is because the method minimises fragmentation and maintains the complete complex by gently ionising molecules in solution. This offers important insights into the structure and stability of metal-ligand complexes by enabling direct observation of their stoichiometry and binding affinities in the gas phase by researchers.

In the present research, Graphene-Oxide has emerged as a promising nano-adsorbent, demonstrating exceptional adsorption capacities compared to other materials. This study aims to delve deeper into the metal-ligand interactions within graphene-Oxide, employing Ionization Mass Spectrometry (MS-ESI) technique for a thorough analysis. By unraveling the intricate details of these interactions, we aim to gain insights into the enhanced adsorption capabilities of graphene-Oxide and further optimize its performance as a highly efficient adsorbent.

The underlying mechanisms responsible for its superior performance, particularly in comparison to other nano-adsorbents, remain to be fully understood. This study employs MS-ESI technique to investigate the metal-ligand interactions within graphene-Oxide-L-Glutamic acid system, aiming to unravel the molecular-level details contributing to its excellent adsorption properties.

The MS-ESI spectrum of Cr (III) ion adsorbed Graphene-Oxide-L-Glutamic acid sample showed significant information about the Ligand-Metal ion interaction during adsorption procedure under aqueous conditions.

In the present study, the base peak was observed at m/z : 590.19 with 100% intensity along with a unique pattern corresponding to Graphene-Oxide (**Figure 5**). The peculiar peak at 434.01 and 435.17 corresponds to the plausible complex formation of $[\text{Cr}(\text{Glu})_2(\text{H}_2\text{O})_3\text{Cl}]$ ($\text{C}_{10}\text{H}_{22}\text{ClCrN}_2\text{O}_{11}$) which might have played a pivotal role in Cr(III) ion adsorption on L-glutamic acid infused Graphene oxide (GO). While isotopic peaks related to $\text{Cr}(\text{III})\text{Cl}_3 \cdot 6\text{H}_2\text{O}$ appeared at 265.09, 267.71, and 269.19 with comparatively lower intensity. This indicates that the adsorption of Cr(III) ions was piloted by Ligand assisted approach with enhanced efficiency.

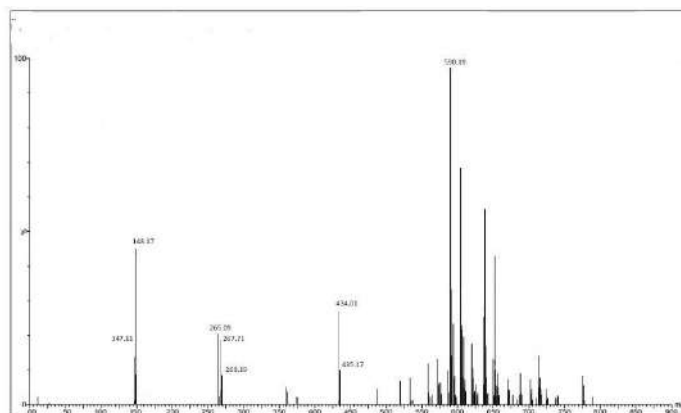


Figure 5. ESI-MS Of L-Glutamic Acid Infused GO-Cr(III)-Adsorbent-Adsorbate Sample.

CONCLUSION

An effective method for adsorbing Cr(III) ions from aqueous samples was to employ naturally occurring organic acid-infused nano-adsorbents. The organic acids that have been infused help to increase adsorption by facilitating ligational interactions with metal ions and chemically binding them to the surface of nano-adsorbents. When compared to non-infused control nano-adsorbents, L-glutamic acid demonstrated increased adsorption up to 8.9% among the natural acid ligands. Because of the reversible metal-ligand interaction that causes the desorption of chromium from the adsorbent up to 139.9 ppm, this unique strategy of ligand-assisted adsorption also offers an efficient method for adsorbent regeneration under heat and electrolytic induction. The metal-ligand interactions are further supported by the mass spectrum analysis, particularly by the peaks at m/z : at 434.01 and 435.17, which greatly facilitates the Cr-L-glutamic acid connections over graphene-oxide. In conclusion, the outlook of the present study helps design and develop efficient strategies for the remediation of Cr(III) contaminants from water samples in the view of human and ecological safeguards.

REFERENCES

- [1] Prasad S, Yadav KK, Kumar S, Gupta N, Cabral-Pinto MMS, Rezania S, Radwan N, Alam J. Chromium contamination and effect on environmental health and its remediation: A sustainable approaches. *Journal of Environmental Management*. 2021; 285(1), 112174. <https://doi.org/10.1016/j.jenvman.2021.112174>
- [2] Singh S, Naik TSSK, Chauhan V, Shehata N, Kaur H, Dhanjal DS, Marcelino LA, Bhati S, Subramanian S, Singh J, Ramamurthy PC. Ecological effects, remediation, distribution, and sensing techniques of chromium. *Chemosphere*. 2022; 135804. <https://doi.org/10.1016/j.chemosphere.2022.135804>.
- [3] Pooja Sharma P, Surendra Pratap Singh SP, Sheetal Kishor Parakh, SK, Yen Wah Tong, YW. Health hazards of hexavalent chromium (Cr (VI)) and its microbial reduction, *Bioengineered*. 2022; 13(3), 4923-4938. <https://doi.org/10.1080/21655979.2022.2037273>
- [4] Irshad MA, Sattar S, Nawaz R, Al-Hussain SA, Rizwan M, Bukhari A, Waseem M, Irfan A, Inam A, Zaki MEA. Enhancing chromium removal and recovery from industrial wastewater using sustainable and

- efficient nanomaterial: A review. *Ecotoxicology and Environmental Safety*. 2023; 263,115231. <https://doi.org/10.1016/j.ecoenv.2023.115231>.
- [5] Saha B, Amine A, Verpoort F. Special Issue: Hexavalent Chromium: Sources, Toxicity, and Remediation. *Chemistry Africa*. 2022;5, 1779–1780. <https://doi.org/10.1007/s42250-022-00443-z>
- [6] Tumolo M, Ancona V, De Paola D, Losacco D, Campanale C, Massarelli C, Uricchio VF. Chromium Pollution in European Water, Sources, Health Risk, and Remediation Strategies: An Overview, *Int. J. Environ. Res. Public Health* 2020, 17, 5438. <https://doi.org/10.3390/ijerph17155438>.
- [7] Al-Battashi H, Joshi S.J, Pracejus, B, Al-Ansari, A. The Geomicrobiology of Chromium (VI) Pollution: Microbial Diversity and its Bioremediation Potential. *TOBIOTJ* 2016; 10, 379–389. <https://doi.org/10.2174/1874070701610010379>.
- [8] Kodiganti S, Kantankar A, Ravinder D, Satyanarayana M, Jonnalagadda SB, Vasam CS. A New Approach for Adsorption of Fe(III) Using Natural Bioorganic Ligands as Facilitating Agents on Selected Adsorbents. *Journal of Water Chemistry and Technology*. 2023, 45, 440–445. <https://doi.org/10.3103/S1063455X23050077>.
- [9] Kumar R, Rauwel P, Rauwel E. Nanoadsorbants for the Removal of Heavy Metals from Contaminated Water: Current Scenario and Future Directions. *Processes*. 2021; 9, 1379. <https://doi.org/10.3390/pr9081379>.
- [10] Tang S, Yang X, Zhang T, Qin Y, Cao C, Shi H, Zhao, Y. Adsorption mechanisms of metal ions (Pb, Cd, Cu) onto polyamide 6 microplastics: New insight into environmental risks in comparison with natural media in different water matrices. *Gondwana Research*. 2022; 110, 214-225. <https://doi.org/10.1016/j.gr.2022.06.017>.
- [11] Priyadarshane M, Das, S. Biosorption and removal of toxic heavy metals by metal tolerating bacteria for bioremediation of metal contamination: A comprehensive review. *Journal of Environmental Chemical Engineering*. 2021; 9(1), 104686. <https://doi.org/10.1016/j.jece.2020.104686>.
- [12] Duan C, Ma, T Wang J, Zhou Y. Removal of heavy metals from aqueous solution using carbon-based adsorbents: A review. *Journal of Water Process Engineering*. 2020; 37, 101339. <https://doi.org/10.1016/j.jwpe.2020.101339>.
- [13] Ferrández-Gómez B, R, Ruiz-Rosas R, Beaumont S, Cazorla-Amorós D, Morallón E. Electrochemical regeneration of spent activated carbon from drinking water treatment plant at different scale reactors. *Chemosphere*. 2021; 264(1), 128399. <https://doi.org/10.1016/j.chemosphere.2020.128399>
- [14] Amin NK, Nosier SA, Abdel-Aziz MH, Hassan MS, Sedahmed GH, El-Naggar MA. Electrochemical regeneration of hexavalent chromium from aqueous solutions in a gas sparged parallel plate reactor. *Environmental Technology*. 2022; 43(16):2405-2417. <https://doi.org/10.1080/09593330.2021.1881827>.